ELSEVIER

Journal of Organometallic Chemistry 630 (2001) 157–168

Journal of Organometallic Chemistry

www.elsevier.com/locate/jorganchem

Molecular modeling of the olefin metathesis by tungsten(0) carbene complexes

Mikhail Tlenkopatchev, Serguei Fomine *

Instituto de Investigaciones en Materiales, Universidad Nacional Autónoma de México, Apartado Postal 70-360, CU, Coyoacán, Mexico DF 04510, Mexico

Received 12 December 2000; received in revised form 1 March 2001; accepted 8 March 2001

Abstract

Density functional and second-order Moller–Plesset theory were used to model W(0) carbene mediated homogeneous metathesis reaction of propylene. The calculations show that the rate determining step of the metathesis is the initiation. After the initiation has been completed the rate determining step becomes dissociation of olefin–metallocarbene complex. The low stereoselectivity of the olefin metathesis reaction is due to the close matching of activation energies for *cis* and *trans* isomer formation and the fast *cis–trans* isomerization caused by the catalysts. The non-productive olefin metathesis reaction always dominates the reaction mixture owing to its very low activation energy. The electronic structure of metal carbene olefin complexes can be described as a combination of donor–acceptor interactions between HOMO of the olefin and LUMO of metal carbene located at carbene carbon on the one hand, and the Dewar, Chatt and Duncanson back donation scheme on the other.

Keywords: Olefin metathesis; Tungsten(0) complexes; DFT calculations; Molecular modeling; Tungsten

1. Introduction

Carbon–carbon bond forming reactions are among the most important family of reactions in organic synthesis. One particularly interesting carbon–carbon bond forming reaction is olefin metathesis, which is the metal-catalyzed exchange of alkylidene moieties between alkenes. Banks and Bailey were the first who observed the metal catalyzed disproportionation of alkenes in 1964 [1]. The olefin metathesis is widely used in industry. One example is the Phillips triolefin process [2], where propylene is converted into a mixture of ethylene and 2-butene. It is generally accepted that the olefin metathesis proceeds via a so-called metal–alkylidene (carbene) chain mechanism first proposed by Herisson and Chuavin [3] (Fig. 1). The propagation reaction involves the transition metal carbene as active species with a vacant coordination site at metal. The olefin coordinates at this vacant site and subsequently a metallacyclobutane intermediate is formed. The metallacyclobutane is unstable and cleaves to form a new metal–carbene complex and a new olefin. This mechanism has been established by numerous investigations [4–8].

The application of the olefin metathesis in organic synthesis has been expanded by the introduction of low valence transition metal carbene [9,10] and stable metal–alkylidene complexes [11–13]. The metal carbene complexes may be prepared as stable compounds at low temperature and cause olefin metathesis [14].

Numerous experimental data showed that Fischer-type W(0) carbene complexes such as $W(=CPh_2)(CO)_5$ can be used as mono-component initiators (without any cocatalysts) in the olefin metathesis [15]. Thus, *cis*- and *trans*-pent-2-ene, pent-1-ene, hex-1-ene, 2-methylpent-1-ene, 2-methylbut-1-ene [16–18], cyclobutene, norbornene and other *cis*-cycloalkenes [19,20] undergo the metathesis in the presence of Fischer-type W(0) carbene complexes. In the case of $W(=CPh_2)(CO)_5$ catalyzed metathesis polymerization of 1-methyl-cyclooctene, diphenylcarbene ($Ph_2C=$) end groups are detected in the polymer [21] giving proof that it is the W(0) complex that initiates the polymerization.

* Corresponding author. Tel. and fax: +52-5616-1201.
E-mail address: fomine@servidor.unam.mx (S. Fomine).

0022-328X/01/$ - see front matter
PII: S0022-328X(01)00932-9

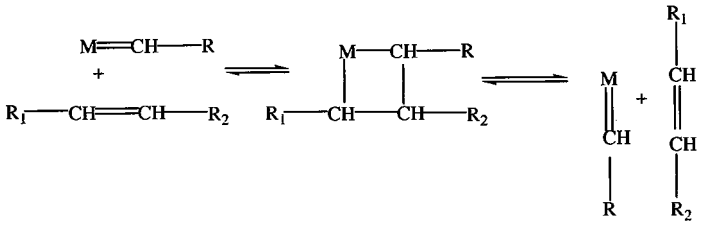

Fig. 1. General mechanism of the olefin metathesis.

In spite of the fact that the olefin metathesis reaction is one of the most studied in organometallic chemistry, there are very few reports dealing with modeling of the metathesis reaction using quantum chemistry tools. Rappé [22] has studied mechanistically the olefin metathesis reaction catalyzed by high-valent Group VI metals. Even though the general features of the metathesis reaction are well established, many important details such as the rate determining step, stereoselectivity, structure of the transition states and olefin–catalyst complexes remain to be studied.

The homogeneous olefin metathesis catalyzed by low valence transition metals is an excellent model reaction for theoretical study. In fact, W(0) carbene complexes are more appropriate model systems to study the metathesis reaction then the classical ones, because the classical metathesis catalysts based on WCl_6 and $MoCl_5$ cause more side reactions then do W(0) carbene complexes. The goal of this paper is to model homogeneous propylene metathesis reaction using pentacarbonyltungsten carbene complex as a model to gain a better understanding of the mechanism of the olefin metathesis reaction.

2. Computational details

The GAUSSIAN 98 program was used for all calculations. Since MP2, B3LYP, and BP86 models perform similarly on the $W(CO)_6$ molecule [23], the BP86 functional was the method of initial choice as less computationally demanding. To test whether the adopted model reproduces adequately the structure of tungsten containing organometallics, the geometry of the recently synthesized ethylene carbonyl tungsten complex [*trans*-$W(CO)_4(\eta^2\text{-}C_2H_4)_2$] [24] was fully optimized at BP86/LANL2DZ level and compared with X-ray crystallography data. The results are shown in Table 1. As can be seen this model correctly reproduces molecular geometry, the W···CO distances were reproduced within 0.01 Å and most of the angles within 2°. Larger errors (0.03 Å) are observed for C–O and ethylene–tungsten distances, however, the overall performance of the model is quite reasonable and, therefore, this model was adopted for all geometry optimizations. All geometries were fully optimized without any symmetry restrictions using Becke's non-local exchange functional [25] and Perdew's non-local [26] correlation functional in combination with LANL2DZ basis set (H (2s), C, O (3s, 2p), W (3s, 3p, 2d + Los Alamos ECP)) [27] using a fine integration grid [28]. Frequency jobs were run for all optimized molecules to ensure that the found stationary point corresponds to either a minimum (zero imaginary frequencies) or transition state (one imaginary frequency). The second-order Moller–Plesset perturbation theory at frozen core approximation was used for single point energy calculations. The same LANL2DZ basis set augmented with polarization functions at heavy atoms was used for these calculations. Due to the fact that postulated intermediates are uncharged and solvents commonly used to carry out the metatheses reactions are aprotic solvents like toluene, it is thought that the solvation barely affects the results of calculations. To test this hypothesis the self-consistent reaction field calculations were carried out for a model metathesis reaction in toluene (Table 2, entries 2, 4, 6) (dielectric constant 2.379) using the gas phase optimized geometries and Onsager's continuum solvation model [29]. As seen from Table 2 (entries 2, 4 and 6) the energy difference between the gas phase and solution calculations barely reach 1 kcal mol^{-1} which is within the range of error produced by the adopted models.

Transition states were located using QST2 or QST3 keywords. The imaginary vibrational modes were carefully analyzed to ensure that the correct transition state was located. Unscaled zero point energies (ZPE) taken from BP86/LANL2DZ frequency jobs were always used to correct the obtained energy in both BP86 and MP2 calculations. As the MP family of methods is sometimes divergent in the case of low lying virtual orbitals, MP4(SDTQ) energies of two W complexes (**Ia** and **II**) were calculated to test the quality of the MP2 method. It was found that E^2, E^3 and E^4 corrections converged for these molecules and therefore MP2 energies can be trusted.

3. Results and discussion

To gain preliminary insight into the olefin metathesis reaction mechanism a simple model of non-productive ethylene metathesis using pentacarbonyltungsten carbene (**I**) as catalyst was studied first (Fig. 2). Since

carbene **I** has no vacant d-orbital to form an olefin complex, one CO molecule must be eliminated to form the olefin complex **II**. There are two possibilities: a synchronic process similar to the S_N2 mechanism and stepwise process similar to the S_N1 mechanism. It seems that the synchronic mechanism can be discarded due to the steric hindrances caused by numerous ligands. The stepwise mechanism shown in Fig. 2 consists in elimination of one CO molecule to give carbene **Ia** having a vacant d-orbital followed by the complexation of ethylene to form olefin complex **II**. The preparation of this type of complex where carbene and olefin form a bidentate ligand after the elimination of one CO molecule has been reported [30]. All efforts to find a transition state corresponding to the complexation–dissociation process have failed and the relaxed potential

Table 1
Bond lengths (Å) and angles (°) for crystalline *trans*-[$W(CO)_4(\eta^2\text{-}C_2H_4)_2$] [a]

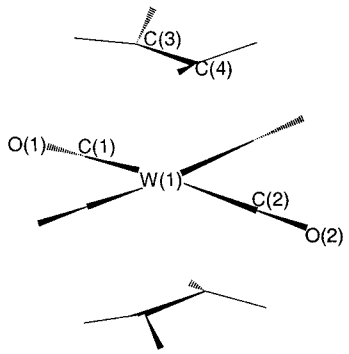

Bond length	Experimental [b]	Calculated [c]	Angle	Experimental [b]	Calculated [c]
W(1)–C(2)	2.033(10)	2.032	C(2)–W(1)–C(2i)	92.3(9)	90.1
W(1)–C(2i)	2.033(10)	2.032	C(2)–W(1)–C(3i)	86.3(4)	87.2
W(1)–C(1)	2.045(9)	2.032	C(2)–W(1)–C(1)	171.8(7)	174.9
W(1)–C(1i)	2.045(9)	2.032	C(2i)–W(1)–C(3i)	111.1(4)	110.3
W(1)–C(4)	2.299(9)	2.360	C(2i)–W(1)–C(1)	90.9(3)	90.1
W(1)–C(4i)	2.299(9)	2.360	C(1)–W(1)–C(3i)	85.5(5)	88.0
W(1)–C(3)	2.315(9)	2.360	C(2)–W(1)–C(1i)	90.9(3)	90.1
W(1)–C(3i)	2.315(9)	2.360	C(1i)–W(1)–C(3i)	76.7(5)	74.8
C(1)–O(1)	1.151(11)	1.196	C(2i)–W(1)–C(1i)	171.8(7)	174.9
C(2)–O(2)	1.142(10)	1.196	C(4)–W(1)–C(3i)	154.8(3)	155.2
C(3)–C(4)	1.413(13)	1.436	C(1)–W(1)–C(1i)	87.0(9)	90.1
			C(4i)–W(1)–C(3i)	35.7(3)	35.4
			C(2)–W(1)–C(4)	75.4(5)	74.9
			C(3)–W(1)–C(3i)	155.4(5)	155.2
			C(2i)–W(1)–C(4)	87.1(5)	88.0
			O(1)–C(1)–W(1)	175.1(13)	179.4
			C(1)–W(1)–C(4)	112.3(5)	110.3
			O(2)–C(2)–W(1)	176.2(14)	179.4
			C(1i)–W(1)–C(4)	86.3(5)	87.2
			C(4)–C(3)–W(1)	71.5(5)	72.3
			C(2)–W(1)–C(4i)	87.1(5)	87.2
			C(2i)–W(1)–C(4i)	75.4(5)	74.8
			C(1)–W(1)–C(4i)	86.3(5)	87.2
			C(1i)–W(1)–C(4i)	112.3(5)	110.3
			C(4)–W(1)–C(4i)	154.9(5)	155.2
			C(2)–W(1)–C(3)	111.1(4)	110.3
			C(3)–C(4)–W(1)	72.8(5)	72.3
			C(2i)–W(1)–C(3)	86.3(4)	88.0
			C(1)–W(1)–C(3)	76.7(5)	74.9
			C(1i)–W(1)–C(3)	85.5(5)	87.2
			C(4)–W(1)–C(3)	35.7(3)	35.4
			C(4i)–W(1)–C(3)	154.8(3)	155.2

[a] Symmetry transformations used to generate equivalent atoms: (i) $1-x, -y, -z$.
[b] From Ref. [24].
[c] BP86/LANL2DZ// BP86/LANL2DZ level of theory.

Table 2
Energetics of the metathesis reactions (kcal mol^{-1})

Reaction	ΔE [a]		E_a [b]		ΔG^{298} [c]
	BP86	MP2	BP86	MP2	
1. **I** → **Ia** + CO	40.5	39.6			
2. **I** → **Ia** + CO(sol)	39.4				
3. **Ia** + C_2H_4 → **II**	−20.8	−37.6			
4. **Ia** + C_2H_4 → **II**(sol)	−20.7				
5. **II** → **II**	0	0	0.03	−0.4	
6. **II** → **II**′(sol)	0	0	−0.2		
7. **V** → **Va** + **CO**	45.1	46.3			
8. **Va** + C_3H_7 → **VI**	−17.4	−42.0			
9. **Va** + C_3H_7 → **VII**	−17.6	−43.4			
10. **VI** → **X**	19.4	25.7	22.4	22.3	18.6
11. **VII** → **XI**	26.6	29.2	29.2	27.2	26.1
12. **X** → **XII** + (OMe)PhC=CH_2	6.8	27.5			
13. **XI** → **XIII** + (OMe)PhC=CH(Me)	7.8	33.2			
14. **XII** + C_3H_7 → **XV**	−14.8	−33.8			
15. **XII** + C_3H_7 → **XIV**	−14.9	−34.1			
16. **XIV** → **XVI**	5.0	1.7	6.0	1.7	6.7
17. **XV** → **XVIII**	3.5	0.3	4.5	0.4	5.1
18. **XVI** → **XVII** + **XXI**	15.4	40.2			
19. **XVIII** → **XIX** + **XX**	15.8	42.3			
20. **XII** + C_3H_7 → **XXII**	−13.7	−34.8			
21. **XII** + C_3H_7 → **XXIII**	−13.6	−35.8			
22. **XXII** → **XXII**	0	0	0.5	0.9	0
23. **XXIII** → **XXIII**	0	0	0.2	−1.0	0
24. **XIII** + C_3H_7 → **XXIV**	−19.6	−39.9			
25. **XXIV** → **XXV**	−1.1	−0.5	0.3	−0.1	−1.9
26. **XXV** → **XII** + C_2H_4	16.8	33.9			
27. **XIII** + C_3H_7 → **XXVI**	−16.7	−37.0			
28. **XXVI** → **XXVI**	0	0	0.7	−0.5	0
29. **XII** + **XX** → **XXVII**	−12.5	−35.1			
30. **XXVII** → **XXVIII**	−0.4	0.5	5.1	1.5	−1.1
31. **XXVIII** → **XII** + **XXI**	13.8	35.8			

[a] Total electronic energy difference + ZPE correction at BP86/LANL2DZ level.
[b] Activation energy including ZPE correction at BP86/LANL2DZ level.
[c] The free Gibbs energy at BP86/LANL2DZ level.

energy scan run for the reactions **I** → **Ia** + CO and **Ia** + ethylene → **II** at BP86/LANL2DZ level of theory gave no maximum energy structure, suggesting that the dissociation–complexation process is thermodynamically controlled. After olefin complex **II** is formed, the reaction passes through a transition state **TrIII** to form a new olefin complex **III**, identical to complex **II** due to the reaction symmetry. Fig. 3 and Table 2 show the geometries and energies of the intermediates involved in the non-productive ethylene metathesis, respectively. As can be seen, MP2 and BP86 levels of theory produce similar results in all cases except for the olefin binding energies where the MP2 model predicts significantly higher stability of the complexes. When BP86 single point energy calculations were rerun with LANL2DZ(d) basis set for the reaction **Ia** + ethylene → **II**, the binding energy found for complex **II** was only 22.7 kcal mol^{-1}, very close to that found for the BP86/LANL2DZ//BP86/LANL2DZ model and different from the energy obtained from MP2 calculations (37.6 kcal mol^{-1}). Therefore, such a difference is related to the method itself not to the basis set. Although, to our knowledge, experimental data dealing with the binding energy of olefin complexes of low valence tungsten carbenes have not been reported, Pidun et al. [31] reported the high quality dissociation energy for $(CO)_5W(C_2H_4)$ complex calculated at CCSD//MP2 level of theory (41.1 kcal mol^{-1}) which is closer to the MP2 energy for complex **II** dissociation (37.6 kcal mol^{-1}) than to the BP86 energy (20.8 kcal mol^{-1}). Additionally, the binding energy in complex **II** was calculated at MP4(SDTQ)/LANL2DZ(d) level using BP86/LANL2DZ optimized geometry. Again, the obtained result (36.1 kcal mol^{-1}) agrees much better with MP2 energies than with BP86 ones. Therefore, the MP2 level seems to be adequate for the energy calculation in this system.

A simple picture of the metathesis reaction indicates that the initiation (formation of intermediate **Ia**) is the rate determining step, while the metathesis reaction itself (**II** → **TrIII**) has very low activation energy of less than 1 kcal mol^{-1}. Once the initiation has been completed the rate determining step becomes the dissociation of olefin–catalyst complex **II** with ΔE of some 20 kcal mol^{-1} (37.6 kcal mol^{-1} for the MP2 model) which is much higher than the activation energy of the metathesis itself and therefore determines the rate of the whole process. As the complexation occurs with no activation energy according to the simulation data, ΔE of dissociation can be considered as the activation energy of the process. Examining the geometries of olefin complex **II** and transition state **TrIII** one can notice their similarity, thus explaining the low activation energy of the reaction. Complex **II** is a tight complex where the formal double bond of ethylene becomes even longer than the single C–C bond of ethane (1.566 versus 1.530 Å, respectively), while the distance between the carbene carbon and the nearest carbon atom of ethylene is 1.712 Å, suggesting strong interactions between these two atoms in complex **II**. The transition state **TrIII** represents a symmetric metallacyclobutane structure with all C–C and W–CH_2 distances of 1.638 and 2.156 Å, respectively.

In the case of propylene metathesis initiated by a 'real' catalyst like the tungsten carbene complex (**V**, Fig. 2) a more complicated picture is observed. Similar to the previous case, the first step should be the dissociation of molecule **V** to generate the intermediate **Va** with vacant d-orbital. Both BP86 and MP2 calculations show that this is an endothermic process with ΔE of 43.0 and 42.1 kcal mol^{-1} respectively (Table 2). It is noteworthy that the values are very close to those obtained for dissociation of simple carbene **I** (Fig. 3).

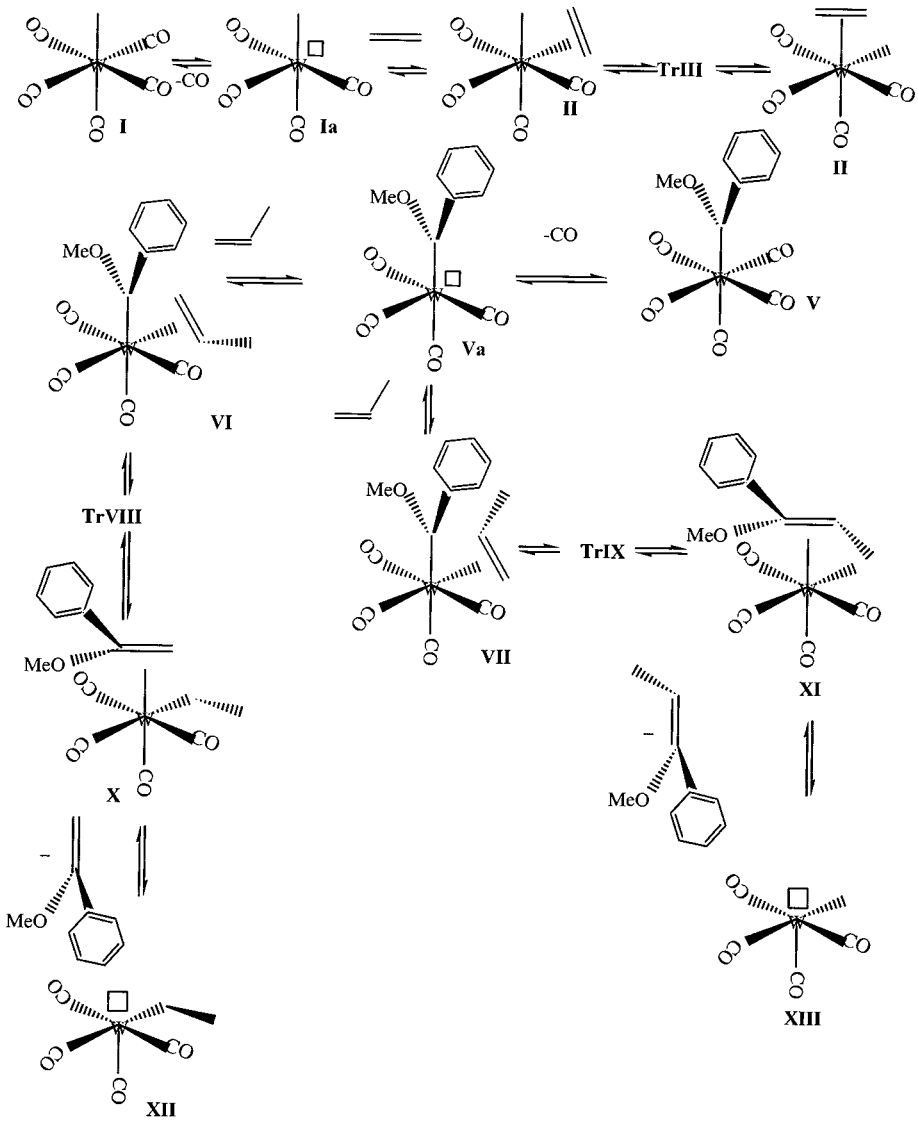

Fig. 2. Model metathesis reaction and the initiation catalyzed by Fisher carbene.

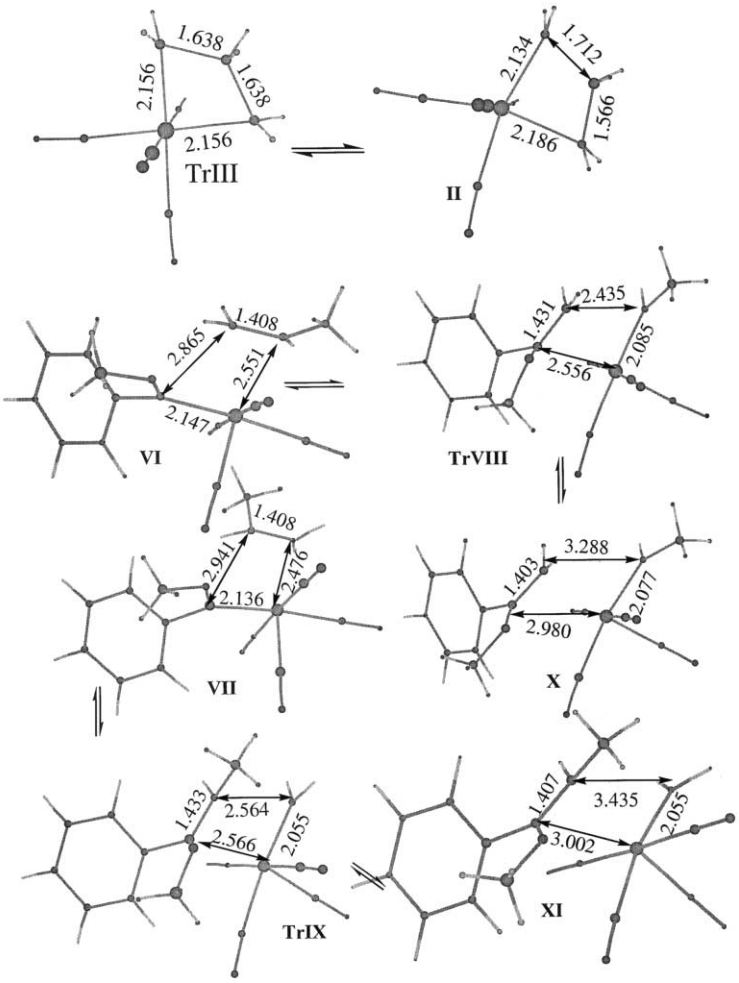

Fig. 3. Geometries and selected bond lengths (Å) of intermediates involved in the model metathesis reaction and initiation step.

Four different olefin–catalyst complexes can be formed on the complexation of **Va** with propylene. Two of them generate primary carbene (**XIII**) as a result of the metathesis and another two produce secondary carbene (**XII**). We will consider only two of four possible structures **VI** and **VII** since the other two structures should be very similar in energy and produce identical carbenes **XII** and **XIII**.

The formation of complexes **VI** and **VII** is an exothermic process similar to the formation of complex **II** with almost identical binding energy (Table 2). As can be seen from Fig. 3, the complexes **VI** and **VII** are much looser than **II**, reflecting both the stabilization of carbene by phenyl and methoxy groups and steric hindrances caused by them. The propylene molecule still maintains its identity with C–C bond length of 1.408 Å in both complexes. The metathesis reaction of complexes **VI** and **VII** leads to the formation of secondary and primary carbene complexes **X** and **XI**, respectively. Both reactions are endothermic with ΔE being more positive for the formation of primary carbene complex at both BP86 and MP2 levels of theory. The activation energy is also higher by 6.8 and 4.9 kcal mol^{-1} for BP86 and MP2 levels of theory, respectively, for the formation of primary carbene complex **XI**, suggesting that formation of the secondary carbene complex **XII** is preferable at the initiation step. The geometries of transition states **TrVIII** and **TrIX** resemble those of complexes **X** and **XI** (Fig. 3) in agreement with Hammond's postulate [32] due to the relatively small energy difference between them. Thus, Ph(OMe)C–CH(CH_3) distances in **TrVIII** and **TrIX** molecules (1.431 and 1.433 Å) are much closer to these for complexes **X** and **XI** (1.403 and 1.407 Å) than to complexes **VI** and **VII** (2.856, 2.941 Å), respectively. Once formed, complexes **X** and **XI** eliminate olefin molecules (1-phenyl-1-methoxyphenyl ethylene and 1-phenyl-1-methoxy-2-methyl ethylene, respectively) to form secondary and primary carbenes **XII** and **XIII**. Again, according to both BP86 and MP2 models, the formation of secondary carbene **XII** is preferably due to the weaker complexation with olefin. Therefore, secondary carbene will dominate the reaction mixture. In accordance to this it has been reported that the α-olefin

metathesis by tungsten(0) carbene complex (Casey carbene) is accompanied by the exchange of methylene groups and this reaction proceeds significantly more rapidly than the metathesis of olefins with internal double bonds [17,18,33]. This means that the metathesis of α-olefin proceeds via secondary carbene complexes. As shown in Ref. [34], the main reaction product of co-metathesis of 1-pentene and 2-butene (equimolar ratios) is propylene, while practically no ethylene is formed. These experimental data demonstrate that under these conditions the reaction proceeds via a secondary carbene complex as energetically the most favorable route in agreement with the results of calculations. Therefore, unsaturated compounds, which form more stable carbene complexes in the metathesis, will retard or completely inhibit the metathesis reaction. This fact explains the lower reactivity of hydrocarbons with conjugated double bonds in metathesis compared with cyclic and linear olefins [35].

Since secondary carbene dominates the reaction, four different pathways should be considered at this stage (Fig. 4). The first two have to do with the productive metathesis reaction to generate *trans*- and *cis*-butene, respectively (Table 2, entries 14, 17, 19 and 15, 16, 18, Fig. 4). The third and the fourth possibilities are the non-productive metathesis to regenerate propylene (Table 2, entries 20, 21, 22, 23, Fig. 3). Fig. 5 shows the geometries of olefin complexes and these of transition states. Two olefin complexes **XIV** and **XV** have similar geometry suggesting that there is no significant steric hindrance between two methyl groups. Moreover, the two complexes have almost identical binding energies according to both MP2 and BP86 models. The transition states, however, leading to the formation of *cis*- and *trans*- butene are distinctly different. The CH(Me)–CH(Me) distance in the **TrXIV** structure is 0.06 Å longer than that of the **TrXV** transition state due to the repulsion of *cis* positioned methyl groups in

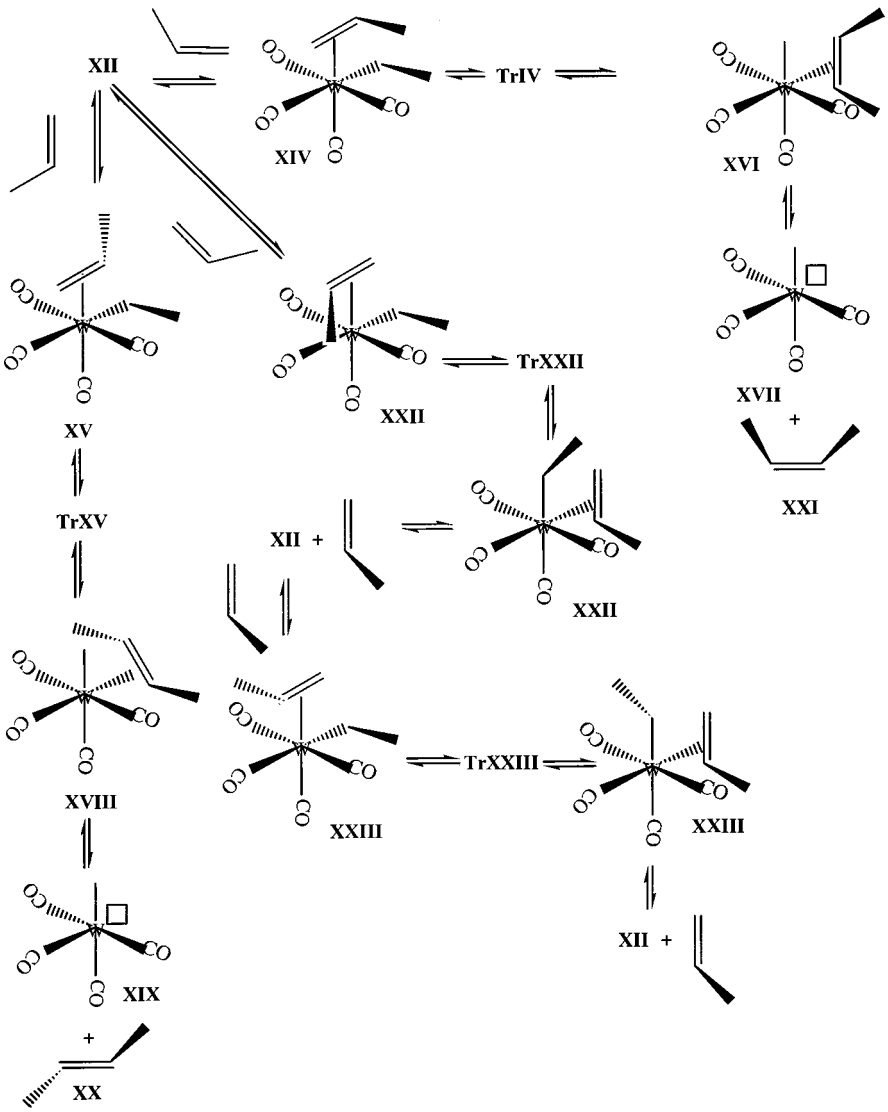

Fig. 4. Propylene metathesis reaction catalyzed by secondary metallocarbene.

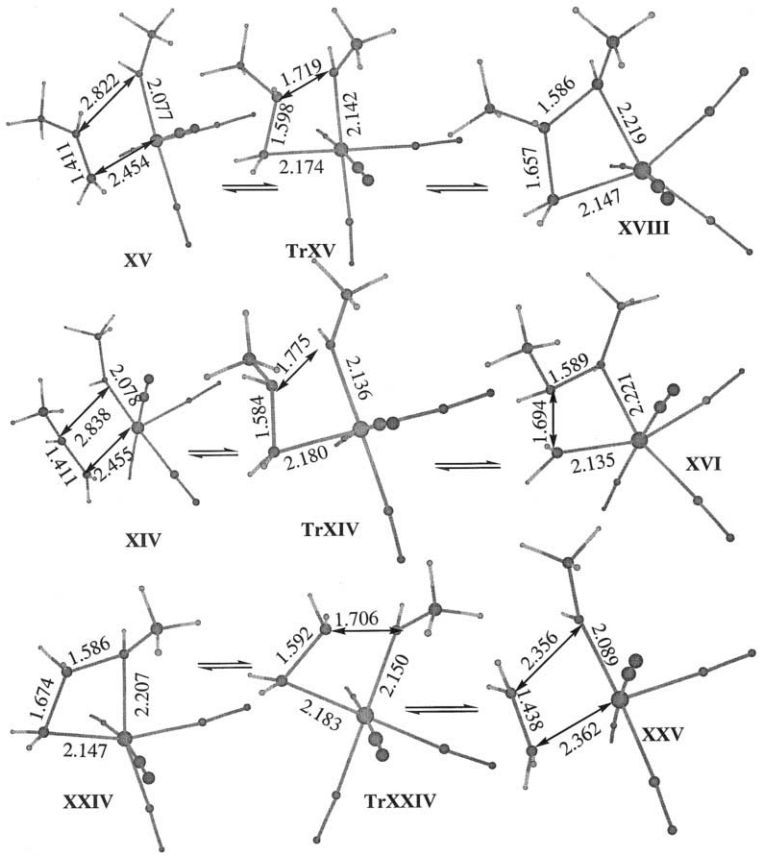

Fig. 5. Geometries and selected bond lengths (Å) of intermediates involved in the metathesis reaction catalyzed by secondary metallocarbene.

the **TrXIV** structure. These steric interactions in the transition state **TrXIV** imply higher activation energy for *cis*-butene formation. The geometries of formed complexes **XVI** and **XVIII** are again similar to one another. The dissociation energy is almost similar at the BP86 level of theory and higher by some 2 kcal mol^{-1} for complex **XVIII** at the MP2 level. As a result, the formations of *cis*- and *trans*-butene are endothermic processes according to both models BP86 and MP2. While according to the BP86 model the formation of *trans*-butene is slightly (1 kcal mol^{-1}) more favorable than that of *cis*-butane, MP2 calculations show exactly the opposite trend. Both models, however, predict a lower by 1.5 kcal mol^{-1} activation energy for *trans*-butene formation.

This finding agrees with the fact that most of the metathesis catalysts show low stereoselectivity with linear olefins. At the final stage of the metathesis, the *trans* to *cis* isomer ratio in the reaction mixture reaches thermodynamic equilibrium due to *cis–trans* isomerization accompanying the olefin metathesis [36,37]. According to BP86 calculations the free Gibbs energy of *cis*-butene → *trans*-butene isomerization is -0.6 kcal mol^{-1} at 298.15 K, corresponding to 73 mol% of *trans*-butene in the equilibrium mixture. This value is very close to the experimentally observed equilibrium *trans* isomer concentration for the internal olefins [38]. The mechanism of *cis–trans* isomerization involves the metathesis on secondary carbene **XII** and the geometry of corresponding complexes and the transition state are shown in Fig. 9. Both BP86 and MP2 models predict low activation energy for this process, being similar to the activation energies of the productive olefin metathesis (Table 2, entry 30), in agreement with the fact that *cis–trans* isomerization occurs during the metathesis of olefins.

The productive metathesis reactions (Table 2, entries 16 and 17) produce primary carbene **XIII** capable of reacting with propylene to give either ethylene (productive metathesis, Table 2, entries 24, 25, 26, Fig. 6) or propylene (non-productive metathesis, Table 2, entries 20, 22, Fig. 5). As can be seen from Table 2, the propylene metathesis giving ethylene is an exothermic reaction, unlike other studied metathesis reactions. Fig. 5 shows the geometry of two olefin complexes (**XXIV** and **XXV**) and the structure of the transition state (**TrXXIV**). The olefin complex **XXIV** is much tighter than **XXV** formed by secondary carbene **XII**, reflecting the lower stability of primary carbene and lesser steric hindrances. This difference in geometries causes the

differences in binding energies of these complexes which are 39.9 and 33.9 kcal mol^{-1} at MP2 level for complexes **XXIV** and **XXV**, respectively. Similar trends maintain at BP86 level. Both levels of theory predict very low activation energy (less than 0.5 kcal mol^{-1}) for this process. Therefore, once formed, primary carbene **XIII** will immediately be converted into secondary carbene **XII** with ethylene formation.

As far as the non-productive metathesis is concerned, three different reactions should be considered. Two of them are the non-productive propylene metathesis on secondary metallocarbene **XII** (Table 2, entries 20–23) and the non-productive propylene metathesis on primary metallocarbene **XIII** (Table 2, entries 27, 28). All other things being equal, the non-productive metathesis dominates the reaction mixture due to low activation energies (less than 1 kcal mol^{-1}).

As can be seen from the above, there is a clear correlation between the $C_{(carbene)}$–$C_{(olefin)}$ equilibrium distances in the olefin–metallocarbene complex and the nature of corresponding metallocarbene (Figs. 3, 5 and 7). The distances increase from primary carbene **XII** to tertiary carbene **Va**. Thus, $C_{(carbene)}$–$C_{(olefin)}$ distances in the complexes formed by propylene and tertiary (**Va**), secondary (**XII**) and primary (**XIII**) metallocarbenes are 2.865, 1.805 and 1.699 Å, respectively. The most obvious reason is steric hindrances increasing from primary to tertiary metallocarbenes. This explanation is not completely satisfactory, however, because in this case one could expect a perceptible C=C bond length difference between ethylene and 1-phenyl-1-methoxyphenyl ethylene. The calculations show, however, that the difference barely reaches 0.01 Å. The electronic factors, therefore, should be of importance in this case. As it has been shown earlier [39], Fisher carbene complexes have the LUMO with largest coefficient at the carbene ligand, while the HOMO has maximum coefficient at the transition metal. Fig. 8 shows LUMOs and HOMOs of secondary metallocarbene **XII** and propylene as an example. As can be seen, the LUMO has a large contribution from the carbene ligand while mainly d-orbitals of tungsten contribute to the HOMO in agreement with previous findings. The formation of olefin complex can be considered in terms of frontier orbital interactions of metallocarbene and olefin. The smaller is the energy gap between the HOMO and LUMO, the stronger are the interactions between the molecules in the complex and, therefore, the shorter is the distance. Other factors to consider are the shape and the symmetry of interacting orbitals. While the LUMO of metallocarbene which has a large contribution from the P_z orbital of carbene carbon can effectively overlap with the HOMO (π-orbital) of the olefin, the overlapping between the HOMO of metallocarbene and the LUMO

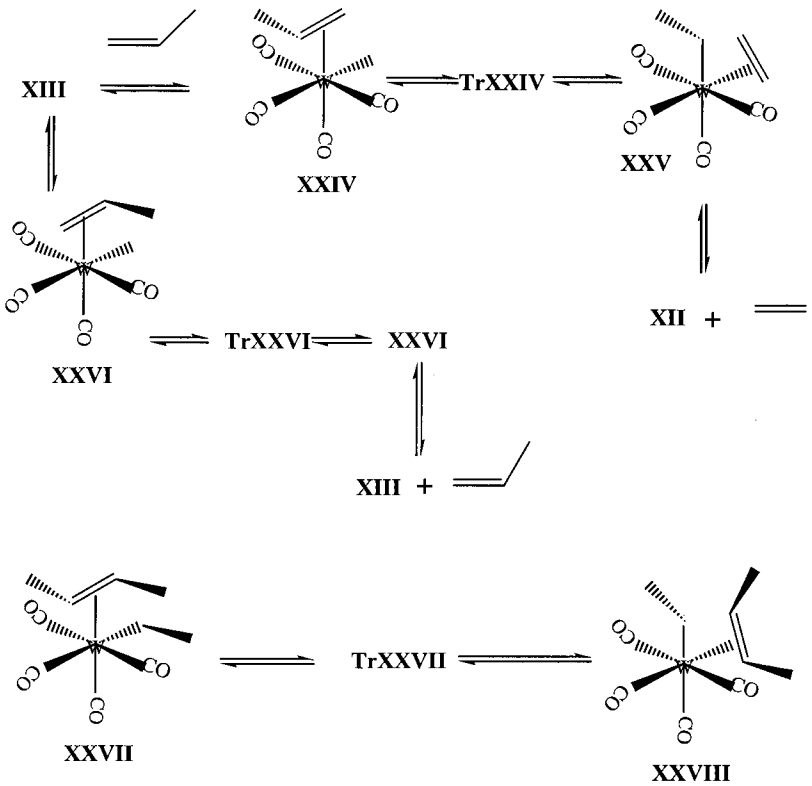

Fig. 6. Propylene metathesis reactions catalyzed by primary metallocarbenecarbene and *cis–trans* isomerization of 2-butene caused by the secondary metallocarbene.

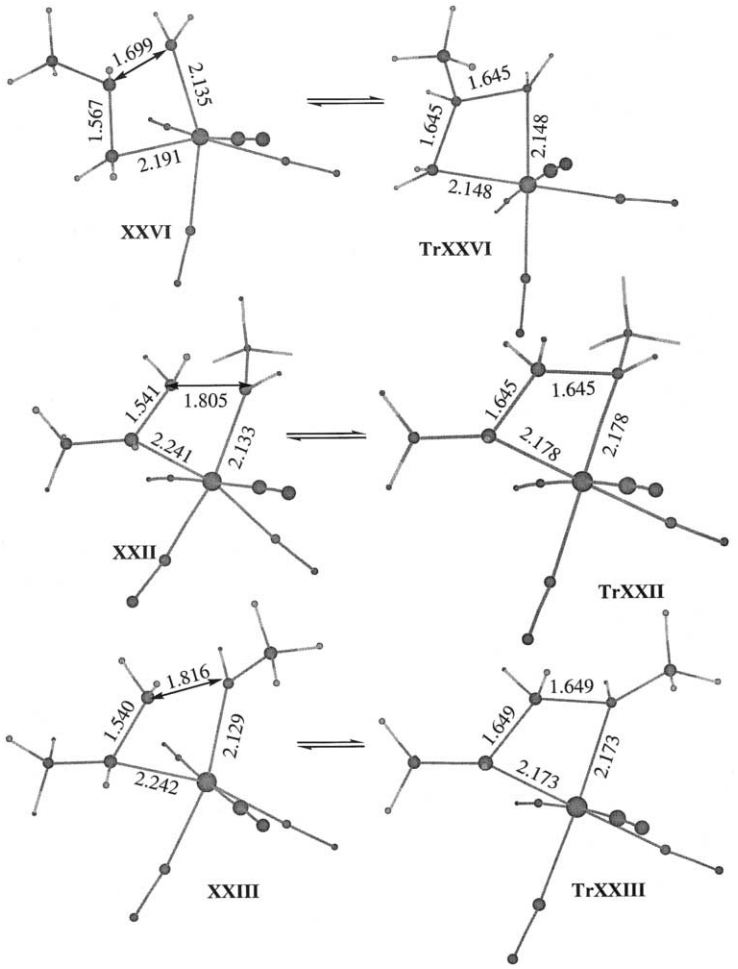

Fig. 7. Geometries and selected bond lengths (Å) of intermediates involved in the non-productive propylene metathesis.

of olefin should be very small due to different symmetry: the LUMO of olefin is a π* orbital while the HOMO of metallocarbene is mainly a $d_{x^2-y^2}$ orbital of tungsten. Table 3 shows the energies of HOMO and LUMO orbitals of metallocarbenes **Va**, **XII** and **XIII**, propylene and ethylene. As can be seen from Table 3, there is a clear correlation between the LUMO (metallocarbene)–HOMO (olefin) energy difference and $C_{(carbene)}-C_{(olefin)}$ distance in complexes **VI**, **XXII** and **XXVI**. The shorter is the distance, the smaller is the LUMO (metallocarbene)–HOMO(olefin) energy difference, reflecting the stronger interaction. Donor substituents at the carbene ligand raise the LUMO energy in secondary **XII** and especially tertiary metallocarbene **Va,** thus increasing the LUMO–HOMO separation. When comparing similar ethylene and propylene complexes (**II** and **XXVI**, **XXV** and **XXII**) one can observe that the $C_{(carbene)}-C_{(olefin)}$ distance is always larger for ethylene complexes which cannot be explained satisfactoryily by steric hindrances. On the other hand, the examination of the HOMO of ethylene and propylene reveals that the HOMO of ethylene is lower in energy and, therefore, interacts more weakly with the LOMO of metallocarbenes explaining the tighter structure of propylene complexes.

The interaction between olefin and carbene in low valent olefin complexes can be described in terms of donor–acceptor interaction. All other things being equal, donor substituents at olefin and acceptor substituents at carbene decrease the energy gap between the HOMO of olefin and the LOMO of metallocarbene, favoring the tight complex formation. The binding energies of olefin–metallocarbene complexes follow this trend (the smaller the $C_{(carbene)}-C_{(olefin)}$ distance the larger the binding energy) with the exception of complexes **VI** and **X** (Table 2). This phenomenon can be understood using the scheme of transition metal (M)–ligand π-back donation [40–42]. According to this scheme the M–ligand bond is not only due to the donation of an electron pair from the HOMO of alkene to the LUMO of the complex but also due to the back donation from the d_{xy} orbital of TM to the LUMO of alkene. When examining the symmetries of molecular orbitals of metallocarbenes **Va**, **XII** and **XIII**, the highest orbital able to overlap with the LUMO of alkene is the HOMO-2 orbital shown in Fig. 8 for the

XII molecule. Owing to the electronodonating groups at carbene ligand, the HOMO-2 has the highest energy in the case of the **Va** molecule (Table 3), thus favoring the effective back donation from TM to alkene. To put it in other words, the high olefin binding energy in complexes **VI** and **X** is due to strong M–olefin interactions.

4. Conclusions

The initiation involving the formation of secondary and primary metal carbenes from olefin–tertiary metal carbene complex is a slow process with high activation energy. The high activation energy of the initiation is due to the stability of tertiary metal carbene.

Once active carbene species have been formed, the rate determining step becomes the dissociation of olefin–metal carbene complex and not the metathesis reaction itself. Both models BP86 and MP2 are in agreement with this trend.

Two factors are responsible for the low stereoselectivity of metathesis catalysts. The first is that the activation energy of the metathesis and the binding energy of olefin–metal carbene complexes are very similar to each other. The second factor is *cis–trans* isomerization taking place during the metathesis reaction: the activation energies of the metathesis and the isomerization

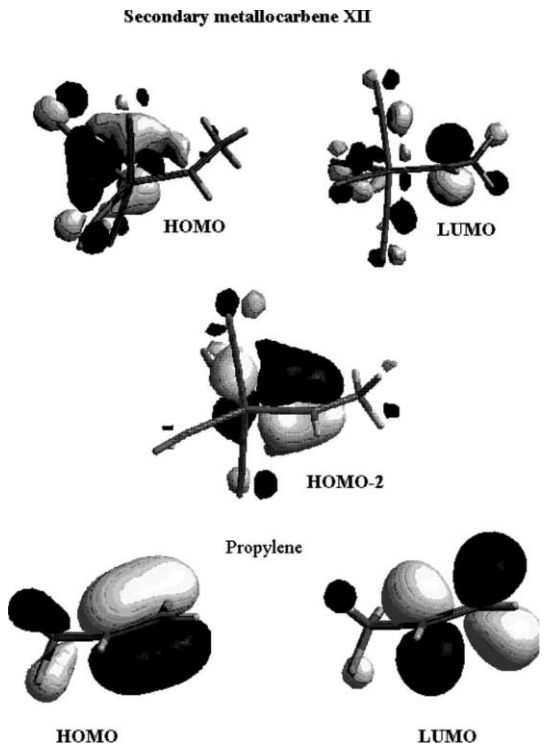

Fig. 8. HOMO, LUMO and HOMO-2 of secondary metallocarbene **XII**. HOMO and LUMO of propylene.

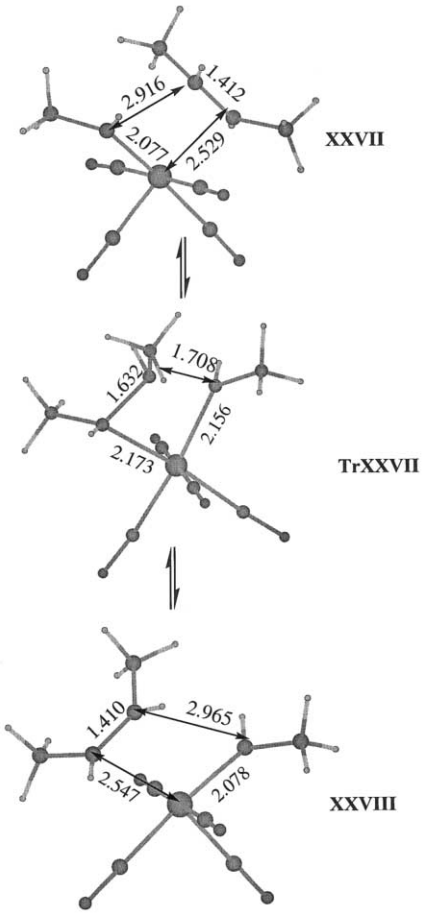

Fig. 9. Geometries of intermediates involved in the secondary metallocarbene mediated *cis–trans* isomerization.

Table 3
MO energies (Hartree) of metallocarbenes **Va**, **XII**, **XIII**, propylene and ethylene calculated at MP2/LANL2DZ(d)//BP86/LANL2DZ level of theory

Molecule	HOMO	LUMO	HOMO-2
Va	−0.28834	0.01343	−0.30894
b	−0.30128	0.01070	−0.35005
XIII	−0.30592	−0.00101	−0.36161
Propylene	−0.35254	0.15852	–
Ethylene	−0.37027	0.14528	–

are very similar leading to equilibrium mixture of the isomers.

The electronic structure of metal carbene olefin complexes can be described as a combination of donor–acceptor interactions between the HOMO of olefin and the LUMO of metal carbene located at carbene carbon on the one hand, and Dewar, Chatt and Duncanson scheme on the other. The former is responsible for the olefin–carbene bonding while the latter accounts for olefin–M interaction.

Acknowledgements

This investigation was supported by grants from CONACyT with contracts 25086A and 32560E.

References

[1] R.L. Banks, G.C. Bailey, Ind. Eng. Chem. Process Des. Dev. 3 (1964) 170.
[2] Phillips Petroleum Company, Hydrocarbon Process, 46 (1967) 232.
[3] J.L. Herisson, Y. Chauvin, Makromol. Chem. 141 (1970) 161.
[4] (a) R.H. Grubbs, P.L. Burk, D.D. Carr, J. Am. Chem. Soc. 97 (1975) 3265;
(b) R.H. Grubbs, D.D. Carr, C. Hoppin, P.L. Burk, J. Am. Chem. Soc. 98 (1976) 3478.
[5] (a) T.J. Katz, J. McGinnis, J. Am. Chem. Soc. 97 (1975) 1592;
(b) T.J. Katz, J. McGinnis, C. Altus, J. Am. Chem. Soc. 98 (1976) 606.
[6] D.J. Cardin, M.C. Doyle, M.F. Lappert, J. Chem. Soc. Chem. Commun. (1972) 927.
[7] (a) B.A. Dolgoplosk, T.G. Golenko, K.L. Makovetsky, I.A. Oreshkin, E.I. Tinyakova, Dokl. Chem. 216 (1974) 807;
(b) B.A. Dolgoplosk, J. Mol. Catal. 15 (1982) 193.
[8] C.P. Casey, R.L. Anderson, J. Chem. Soc. Chem. Commun. (1975) 895.
[9] (a) E.O. Fischer, A. Maasbol, Angew. Chem. 3 (1964) 580;
(b) R. Aumann, E.O. Fischer, Angew. Chem. 79 (1967) 900.
[10] (a) C.P. Casey, T.J. Burkhardt, J. Am. Chem. Soc. 95 (1973) 5833;
(b) C.P. Casey, L.D. Albin, T.J. Burkhardt, J. Am. Chem. Soc. 99 (1979) 2533.
[11] (a) C.J. Schaverien, J.C. Dewan, R.R. Schrock, J. Am. Chem. Soc. 108 (1986) 2771;
(b) R.R. Schrock, J. Feldman, L.F. Cannitzo, R.H. Grubbs, Macromolecules 20 (1987) 1172;
(c) R.R. Schrock, S.A. Krouse, K. Knoll, J. Feldman, J.C. Murdzek, D.C. Yang, J. Mol. Catal. 46 (1988) 243.
[12] (a) J. Kress, J.A. Osborn, V. Amir-Ebrahimi, K.J. Ivin, J.J. Rooney, J. Chem. Soc. Chem. Commun. (1988) 1164;
(b) K.J. Ivin, J. Kress, J.A. Osborn, J. Mol. Catal. 46 (1988) 351;
(c) R.M.E. Greene, K.J. Ivin, J.J. Rooney, J. Kress, J.A. Osborn, Makromol. Chem. 189 (1988) 2797.
[13] (a) S.T. Nguyen, L.K. Johnson, R.H. Grubbs, J. Am. Chem. Soc. 114 (1992) 3974;
(b) S.T. Nguyen, R.H. Grubbs, J.W. Ziller, J. Am. Chem. Soc. 115 (1993) 9858;
(c) P. Schwab, M.B. France, J.W. Ziller, R.H. Grubbs, Angew. Chem. Int. Ed. Engl. 34 (1995) 2039.
[14] T.J. Katz, T.M. Sivavec, J. Am. Chem. Soc. 107 (1985) 737.
[15] K.J. Ivin, J.C. Mol, Olefin Metathesis and Metathesis Polymerization, Academic Press, San Diego, CA, 1997, chapters 2, 3, 6, 7, 9.
[16] T.J. Katz, W.H. Hersh, Tetrahedron Lett. (1977) 585.
[17] C.P. Casey, H.E. Tuinstra, M.C. Saeman, J. Am. Chem. Soc. 98 (1976) 608.
[18] J McGinnis, T.J. Katz, S. Hurwitz, J. Am. Chem. Soc. 98 (1976) 605.
[19] T.J. Katz, S.E. Lee, N. Acton, Tetrahedron Lett. (1976) 4247.
[20] T.J. Katz, N. Acton, Tetrahedron Lett. (1976) 4251.
[21] S.J. Lee, J. McGinnis, T.J. Katz, J. Am. Chem. Soc. 98 (1976) 7818.
[22] A.K. Reppe, W. Goddard, J. Am. Chem. Soc. 104 (1982) 448.
[23] R.K Szilagyi, G. Frenking, Organometallics 16 (1997) 4807.
[24] T. Szymanska-Buzar, K. Kern, A.J. Downs, T.M. Greene, L.J. Morris, S. Parsons, New J. Chem. 23 (1999) 407.
[25] A.D. Becke, Phys. Rev. A 38 (1988) 3098.
[26] (a) J.P. Perdew, Phys. Rev. B 33 (1986) 8822;
(b) J.P. Perdew, Phys. Rev. B 34 (1986) 7406.
[27] P.J. Hay, W.R. Wadt, J. Chem. Phys. 82 (1985) 270.
[28] M.J. Frisch, G.W. Trucks, H.B. Schlegel, G.E. Scuseria, M.A. Robb, J.R. Cheeseman, V.G. Zakrzewski, J.A. Montgomery, Jr., R.E. Stratmann, J.C. Burant, S. Dapprich, J.M. Millam, A.D. Daniels, K.N. Kudin, M.C. Strain, O. Farkas, J. Tomasi, V. Barone, M. Cossi, R. Cammi, B. Mennucci, C. Pomelli, C. Adamo, S. Clifford, J. Ochterski, G.A. Petersson, P.Y. Ayala, Q. Cui, K. Morokuma, D.K. Malick, A.D. Rabuck, K. Raghavachari, J.B. Foresman, J. Cioslowski, J.V. Ortiz, B.B. Stefanov, G. Liu, A. Liashenko, P. Piskorz, I. Komaromi, R. Gomperts, R.L. Martin, D.J. Fox, T. Keith, M.A. Al-Laham, C.Y. Peng, A. Nanayakkara, C. Gonzalez, M. Challacombe, P.M.W. Gill, B. Johnson, W. Chen, M.W. Wong, J.L. Andres, C. Gonzalez, M. Head-Gordon, E.S. Replogle, J.A. Pople, GAUSSIAN 98, Revision A.3, Gaussian, Inc., Pittsburgh, PA, 1998.
[29] M.W. Wong, M.J. Frisch, K.B. Wiberg, J. Am. Chem. Soc. 113 (1991) 4776.
[30] C.P. Casey, A.J. Shusterman, J. Mol. Catal. 8 (1980) 1.
[31] U. Pidun, G. Frenking, J. Organomet. Chem. 525 (1996) 269.
[32] G. Hammond, J. Am. Chem. Soc. 77 (1955) 334.
[33] C.P. Casey, T.L. Burkhardt, J. Am. Chem. Soc. 96 (1974) 7808.
[34] (a) B.A. Dolgoplosk, E.I. Tinyakova, V.A. Yakavlev, Dokl. Chem. 232 (1977) 1075;
(b) I.A. Oreshkin, B.A. Dolgoplosk, E.I. Tinyakova, K.L. Makovetskii, Dokl. Chem. 228 (1976) 1351.
[35] (a) Yu.V. Korshak, M.A. Tlenkopatchev, B.A. Dolgoplosk, E.G. Avdeikina, D.F. Kutepov, J. Mol. Catal. 15 (1982) 207;
(b) M.A. Tlenkopachev, Yu.V. Korshak, A.V. Orlov, V.V. Korshak, Dokl. Chem. 291 (1986) 409.
[36] (a) M. Leconte, J.M. Basset, J. Am. Chem. Soc. 101 (1979) 7296;
(b) N. Taghizadeh, F. Quignard, M. Leconte, J.M. Basset, C. Larroche, J.P. Laval, A. Lattes, J. Mol. Catal. 15 (1982) 219.
[37] (a) M.A. Tlenkopachev, I.A. Kop'eva, Yu.V. Korshak, E.I. Tinyakova, B.A. Dolgoplosk, Dokl. Chem. 227 (1976) 889;
(b) Yu.V. Korshak, B.A. Dolgoplosk, M.A. Tlenkopachev, Rec. Trav. Chim. Pays-Bas 96 (1977) M64.
[38] I.A. Kop'eva, E.I. Tinyakova, B.A. Dolgoplosk, Vysokomolek. Soed. 11B (1969) 717. L.M. Vardanyan, Yu.V. Korshak, M.P. Teterina, B.A. Dolgoplosk, Dokl. Chem. 207 (1972) 345.
[39] (a) H. Nakatsuji, J. Ushio, S. Han, T. Yonezawa, J. Am. Chem. Soc. 105 (1983) 426;
(b) J. Ushio, H. Nakatsuji, T. Yonezawa, J. Am. Chem. Soc. 106 (1984) 5892.
[40] E.R. Davidson, K.L. Kunze, F.B.C. Machado, S. Chakravorty, J. Acc. Chem. Res. 26 (1993) 628.
[41] K.L. Kunze, E.R. Davidson, J. Phys. Chem. 96 (1992) 2129.
[42] F.B.C. Machado, E.R. Davidson, J. Phys. Chem. 97 (1993) 4397.